MODELLING THE LIGHT FIELD IN MACROALGAE AQUACULTURE

A Thesis

Presented to

The Graduate Faculty of The University of Akron

In Partial Fulfillment

of the Requirements for the Degree

Master of Science

Oliver Graham Evans

May, 2018

MODELLING THE LIGHT FIELD IN MACROALGAE AQUACULTURE

Oliver Graham Evans

Thesis

Approved:

Advisor
Dr. Kevin Kreider

Co-Advisor
Dr. Curtis Clemons

Faculty Reader
Dr. Gerald Young

Department Chair
Dr. Kevin Kreider

Accepted:

Dean of the College
Dr. John Green

Dean of the Graduate School
Dr. Chand Midha

Date

ABSTRACT

A probabilistic model for the spatial distribution of kelp fronds is developed based on a kite-shaped geometry and simple assumptions about the motion of fronds due to water velocity. Radiative transfer theory is then applied to determine the radiation field by using the kelp model to determine optical properties of the medium. Finite difference and asymptotic solutions are explored, and behavior of the results over the parameter space is investigated. Numerical simulations to predict the lifetime biomass production of kelp plants are performed to compare our light model to the previous exponential decay model.

Acknowledgments: This project was supported in part by the National Science Foundation under Grant No. EEC-1359256, and by the Norwegian National Research Council, Project number 254883/E40.

Mentors: Shane Rogers, Department of Environmental Engineering, Clarkson University; Ole Jacob Broch, and Aleksander Handå, SINTEF Fisheries and Aquaculture, Trondheim, Norway.

TABLE OF CONTENTS

LIST OF TABLES

LIST OF FIGURES

CHAPTER I

INTRODUCTION

1.1 Motivation

Given the global rise in population, efficient and innovative resource utilization is increasingly important. In particular, food and fuel are clearly in high demand. Meanwhile, growing concern for the negative environmental impacts of petroleum-based fuel is generating a market for biofuel, especially corn-based ethanol. However, corn-based ethanol has been heavily criticized for diverting land usage away from food production. At the same time, a great deal of unutilized saltwater coastline is available for both food and fuel production through seaweed cultivation. Specifically, the sugar kelp *Saccharina Latissima* is known to be a viable source of food, both for direct human consumption and for fish cultivation, as well as for biofuel production.

Furthermore, nitrogen leakage into water bodies is a significant ecological danger, and is especially relevant near large conventional agriculture facilities due to run-off from nitrogen-based fertilizers, as well as near wastewater treatment plants. As a specific example, there is a wastewater treatment plant in Boothbay Harbor, Maine which is facing increasingly demanding EPA regulations limiting the concentration of certain nutrients permissible to be released into the ocean via wastewater

treatment outfalls. In order to adhere to these stricter requirements using conventional nutrient remediation, a significant quantity of specialized equipment would be necessary, which is not currently present in the Boothbay Harbor plant. Being surrounded on all sides by water and private property, the treatment plant lacks the necessary space for the additional equipment, and would therefore need to move their entire facility to a new location in order to conform to these new nutrient regulations. As an alternative to conventional nutrient remediation techniques, the cultivation of the macroalgae *Saccharina Latissima* (sugar kelp) near the outfall site has been proposed. The purpose of such an undertaking would be twofold: to prevent eutrophication of the surrounding ecosystem by sequestering the nutrients in question, and to reduce the need for nutrient input, which is one of the largest costs in macroalgae cultivation.

Once grown, a variety of products can be derived from macroalgae, including biofuel, fish/cattle feed stock, and high value chemical materials such as alginate and agar. Food for human consumption is also a common product of kelp aquaculture, though it may not be ideal for a wastewater treatment application. Thus, there is an ongoing effort to investigate the feasibility, and optimal implementation of kelp farming in wastewater treatment operations.

Industrial scale macroalgae cultivation has long existed in Eastern Asia due to the popularity of seaweed in Asian cuisine. More recently, kelp aquaculture has been developing in Scandinavia and in the Northeastern United States. For example, the MACROSEA project is a four year international research collaboration funded by

the Research Council of Norway targeting "successful and predictable production of high quality biomass thereby making significant steps towards industrial macroalgae cultivation in Norway." The project includes both cultivators and scientists, working to develop a precise understanding of the full life cycle of kelp and its interaction with its environment. A fundamental aspect of this endeavor is the development of mathematical models to describe the growth of kelp. Work is underway at SINTEF, a private Norwegian research institution, to develop such models. Ole Jacob Broch is a mathematician at SINTEF, a research organization in Trondheim, Norway, who has been working to model the growth of *Saccharina Latissima* using SINMOD, a large-scale 3D hydrodynamical ocean model developed at SINTEF which generates data on water temperature, water velocity, light intensity, and phytoplankton concentrations among other valuable quantities [12].

One aspect of the model which has yet to be fully developed is the availability of light, considering factors such as absorption and scattering by the aquatic medium, as well as by the kelp itself. In this thesis, we contribute to this effort by developing a first-principles model of the light field in a kelp farming environment. As a first step, a model for the spatial distribution of kelp is developed. Radiative transfer theory is then applied to determine the effects of the kelp and water on the availability of light throughout the medium. We pursue a numerical finite difference solution to the Radiative Transfer Equation, and subsequently discuss asymptotic approximations which prove to be sufficiently accurate and less computationally intensive. We also provide a detailed description of the numerical solution of this model, accompanied

by source code for a FORTRAN implementation of the solution. This model can be used independently, or in conjunction with a life cycle kelp model to determine the amount of light available for photosynthesis at a single time step.

Figure 1.1: *Saccharina Latissima* being harvested

1.2 Background on Kelp Models

Mathematical modeling of macroalgae growth is not a new topic, although it is a reemerging one. Several authors in the second half of the twentieth century were interested in describing the growth and composition of the macroalgae *Macrocystis pyrifera*, commonly known as "giant kelp," which grows prolifically off the coast

of southern California. The first such mathematical model was developed by W.J. North for the Kelp Habitat Improvement Project at the California Institute of Technology in 1968 using seven variables. By 1974, Nick Anderson greatly expanded on North's work, and created the first comprehensive model of kelp growth which he programmed using FORTRAN [1]. In his model, he accounts for solar radiation intensity as a function of time of year and time of day, and refraction on the surface of the water. He uses a simple model for shading, simply specifying a single parameter which determines the percentage of light which is allowed to pass through the kelp canopy floating on the surface of the water. He also accounts for attenuation due to turbidity using Beer's Law. Using this data on the availability of light, he calculates the photosynthesis rates and the growth experienced by the kelp.

Over a decade later in 1987, G.A. Jackson expanded on Anderson's model for *Macrocystis pyrifera*, with an emphasis on including more environmental parameters and a more complete description of the growth and decay of the kelp [7]. He takes into account respiration, frond decay, and most importantly for my work, sub-canopy light attenuation due to self-shading. He simply adds a coefficient to the exponential decay of light as a function of depth to represent shading from kelp fronds. He doesn't consider and radial nor angular dependence on shading. Jackson also expands Anderson's definition of canopy shading, treating the canopy not as a single layer, but as 0, 1, or 2 discrete layers, each composed of individual fronds. While this is a significant improvement over Anderson's light model, it is still rather simplistic.

Both Anderson's and Jackson's model were carried out by numerically solving a system of differential equations over small time intervals. In 1990, M.A. Burgman and V.A. Gerard developed a stochastic population model [3]. This approach is quite different, and functions by dividing kelp plants into groups based on size and age, and generating random numbers to determine how the population distribution over these groups changes over time, based on measured rates of growth, death, decay, light availability, etc. That same year, Nyman et. al. tested a similar model in New Zealand, as well as a Markov chain model, and compared the results with experimental data [9].

In 1996 and 1998 respectively, P. Duarte and J.G. Ferreira used the size-class approach to create a more general model of macroalgae growth, and Yoshimori et. al. created a differential equation model of *Laminaria religiosa* with specific emphasis on temperature dependence of growth rate [5, 13]. These were the some of the first models of kelp growth that did not specifically relate to *Macrocystis pyrifera* ("giant kelp"). Initially, there was a great deal of excitement about this species due to it's incredible size and growth rate, but difficulties in harvesting and negative environmental impacts have caused scientists to investigate other kelp species.

1.3 Background on Radiative Transfer

In terms of optical quantities, our primary interest is in the radiance at each point from all directions, which affects the photosynthetic rate of the kelp, and therefore the total amount of biomass producible in a given area as well as the total nutrient remediation potential. The equation governing the radiance throughout the system is known as the Radiative Transfer Equation (RTE), which has been largely unutilized in the fields of oceanography and aquaculture. Meanwhile, it has been studied extensively in two fields: stellar astrophysics and computer graphics. In its full form, radiance is a function of 3 spatial dimensions, 2 angular dimensions, and frequency, making for an incredibly complex problem. In this work, frequency is ignored, only monochromatic radiation is considered. The RTE states that along a given path, radiance is decreased by absorption and scattering out of the path, while it is increased by emission and scattering into the path. In our situation, emission is negligible, owing only perhaps to some small luminescent phytoplankton or some such anomaly, and can therefore be safely ignored.

We use monochromatic radiative transfer in order to model the light field in an aqueous environment populated by vegetation. The vegetation (kelp) is modeled by a spatial probability distribution, which we assume to be given. The two quantities we seek to compute are *radiance* and *irradiance*. Radiance is the intensity of light in at a particular point in a particular direction, while irradiance is the total light intensity at a point in space, integrated over all angles. The Radiative Transfer

Equation is an integro-partial differential equation for radiance, which has been used primarily in stellar astrophysics; it's application to marine biology is fairly recent [8].

Understanding the growth rate and nutrient recovery by kelp cultures has important marine biological implications. For example, recent work by our research group at Clarkson University, the University of Maine, and SINTEF Fisheries and Aquaculture is investigating kelp aquaculture as a means to recover nutrients from wastewater effluent plumes in coastal environments into a valuable biomass feedstock for many products. Current models for kelp growth place little emphasis on the way in which nearby plants shade one another. Self-shading may be a significant model feature, though, as light availability may impact the growth and composition of the kelp biomass, and thus the mixture of goods that may be derived.

1.4 Summary of Main Results

CHAPTER II

KELP MODEL

2.1 Physical Setup

Being a salt water species, macroalgae cultivation occurs primarily in the ocean, with the exception of the initial stage of growth, where microscopic kelp spores are inoculated onto a thread in a small laboratory pool. This thread is then wrapped around a large rope, which is placed in the ocean and generally suspended by buoys in one of two configurations: horizontal or vertical. Thus far, I am primarily concerned with modeling the vertical rope case, in which the kelp plants extend radially outward from the rope in all directions, which are made up of a single frond (leaf), stipe (stem) and holdfast (root structure). We consider a rectangular grid of such vertical ropes. Plants extending from each rope will shade both themselves and their neighbors to varying degrees based on the depth of the kelp, the rope spacing, the angle of incident light on the surface and the nature of scattering in the water. In addition, light will be naturally absorbed by the water to varying degrees as determined by the clarity of the water.

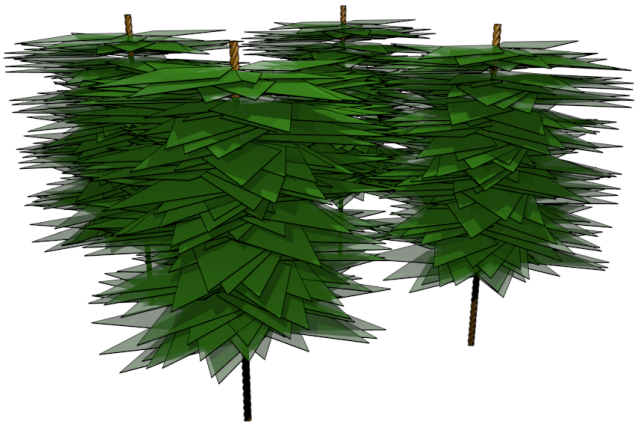

Figure 2.1: 4×4 array of vertical kelp ropes

2.1.1 Coordinate System

Consider the rectangular domain

$$x_{\min} \leq x \leq x_{\max},$$

$$y_{\min} \leq y \leq y_{\max},$$

$$z_{\min} \leq z \leq z_{\max}.$$

For all three dimensional analysis, we use the absolute coordinate system defined in figure 2.2. In the following sections, it is necessary to convert between Cartesian and spherical coordinates, which we do using the relations

$$\begin{aligned} x &= r \sin\phi \cos\theta, \\ y &= r \sin\phi \sin\theta, \\ z &= r \cos\phi. \end{aligned} \tag{2.1}$$

Therefore, for some function $f(x, y, z)$, we can write its derivative along a path in spherical coordinates in terms of Cartesian coordinates using the chain rule.

$$\frac{\partial f}{\partial r} = \frac{\partial f}{\partial x}\frac{\partial x}{\partial r} + \frac{\partial f}{\partial y}\frac{\partial y}{\partial r} + \frac{\partial f}{\partial z}\frac{\partial z}{\partial r} \tag{2.2}$$

Then, calculating derivatives from (2.1) yields

$$\frac{\partial f}{\partial r} = \frac{\partial f}{\partial x}\sin\phi\cos\theta + \frac{\partial f}{\partial y}\sin\phi\sin\theta + \frac{\partial f}{\partial z}\cos\phi. \tag{2.3}$$

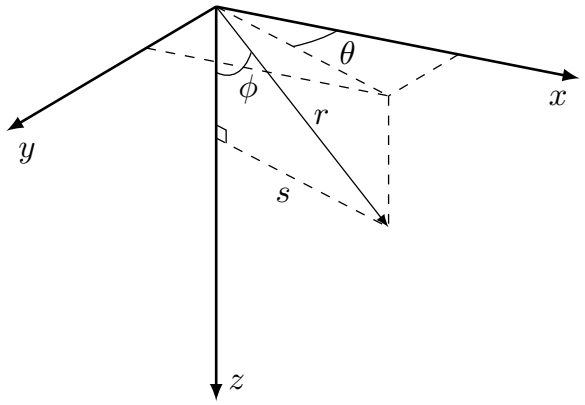

Figure 2.2: Downward-facing right-handed coordinate system with radial distance r from the origin, distance s from the z axis, zenith angle ϕ and azimuthal angle θ

2.2 Kelp Model

2.2.1 Frond shape

We assume the frond is a kite with length l from base to tip, and width w from left to right. The shortest distance from the base to the diagonal connecting the left and right corners is called f_a, and the shortest distance from that diagonal to the tip is

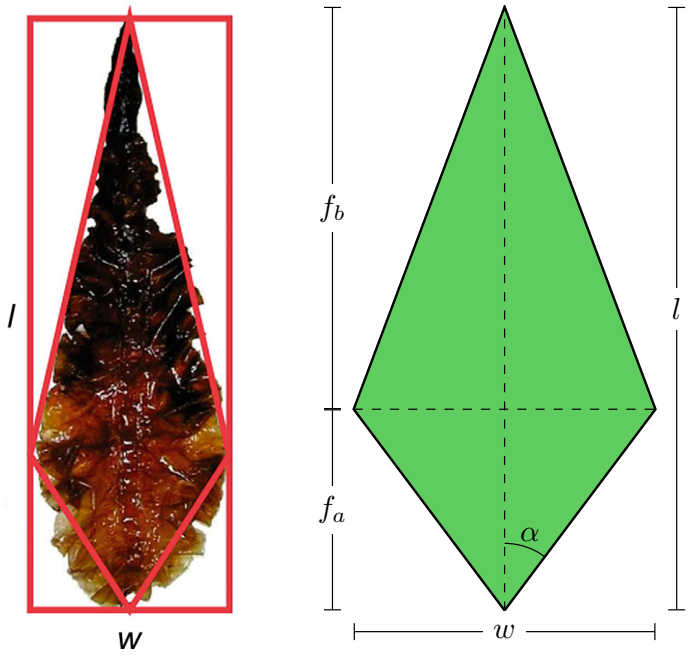

Figure 2.3: Simplified kite-shaped frond

called f_b. We have

$$f_a + f_b = l \tag{2.4}$$

When considering a whole population with varying sizes, it is more convenient to specify ratios than absolute lengths. Let the following ratios be defined.

$$f_r = \frac{l}{w} \tag{2.5}$$

$$f_s = \frac{f_a}{f_b} \tag{2.6}$$

These ratios are assumed to be consistent among the entire population, making all fronds geometrically similar. With these definitions, the shape of the frond can be fully specified by l, f_r, and f_s. It is possible, then, to redefine w, f_a and f_b as follows from the preceding formulas.

$$w = \frac{l}{f_r} \tag{2.7}$$

$$f_a = \frac{l f_s}{1 + f_s} \tag{2.8}$$

$$f_b = \frac{l}{1 + f_s} \tag{2.9}$$

The angle α, half of the angle at the base corner, is also important in our analysis. Using the above equations,

$$\alpha = \tan^{-1}\left(\frac{2 f_r f_s}{1 + f_s}\right) \tag{2.10}$$

The area of the frond is given by

$$A = \frac{lw}{2} = \frac{l^2}{2 f_r}. \tag{2.11}$$

Likewise, if the area is known, then the length is

$$l = \sqrt{2 A f_r} \tag{2.12}$$

2.2.2 Length and angle distributions

We assume that frond lengths are normally distributed with mean μ_l and standard deviation σ_l. We assume the frond angle varies according to the von Mises distribution, which is the periodic analogue of the normal distribution, defined on $[-\pi, \pi]$ rather than $(-\infty, \infty)$. The von Mises distribution has two parameters, μ and κ, which shift and sharpen its peak respectively, as shown in Figure 2.4. κ can be considered analogous to $1/\sigma$ in the normal distribution. Here, we use $\mu = \theta_w$ and $\kappa = v_w$. That is, in the case of zero current velocity, the frond angles are be distributed uniformly,

while as current velocity increases, they become increasingly likely to be pointing in the direction of the current. Note that θ_w and v_w vary over depth.

The PDF for this distribution is

$$P_{\theta_f}(\theta_f) = \frac{\exp\left(v_w \cos(\theta_f - v_w)\right)}{2\pi I_0(v_w)} \tag{2.13}$$

where $I_0(x)$ is the modified Bessel function of the first kind of order 0. Notice that unlike the normal distribution, the von Mises distribution approaches a *non-zero* uniform distribution as κ approaches 0.

$$\lim_{v_w \to 0} P_{\theta_f}(\theta_f) = \frac{1}{2\pi} \; \forall \, \theta_f \in [-\pi, \pi] \tag{2.14}$$

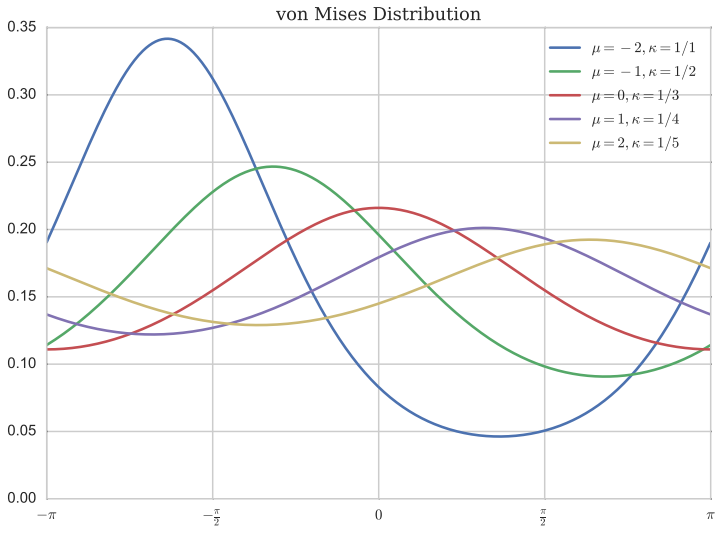

Figure 2.4: von Mises distribution for a variety of parameters

2.2.3 Combined 2D length-angle distribution

The previous two distributions can reasonably be assumed to be independent of one another. That is, the angle of the frond does not depend on the length, or vice versa. Therefore, the probability of a frond simultaneously having a given frond length and angle is the product of their individual probabilities.

Given independent events A and B,

$$P(A \cap B) = P(A)P(B) \tag{2.15}$$

Then the probability of frond length l and frond angle θ_f coinciding is

$$P_{2D}(\theta_f, l) = P_{\theta_f}(\theta_f) \cdot L(l) \tag{2.16}$$

A contour plot of this 2D distribution for a specific set of parameters is shown in figure 2.5, where probability is represented by color in the 2D plane. Darker green represents higher probability, while lighter beige represents lower probability. In figure 2.6, 50 samples are drawn from this distribution and plotted.

It is important to note that if P_{θ_f} were dependent on l, the above definition of P_{2D} would no longer be valid. For example, it might be more realistic to say that larger fronds are less likely to bend towards the direction of the current. In this case, (2.15) would no longer hold, and it would be necessary to use the following more general relation.

$$P(A \cap B) = P(A)P(B|A) = P(B)P(B|A) \tag{2.17}$$

This is currently not taken into consideration in this model.

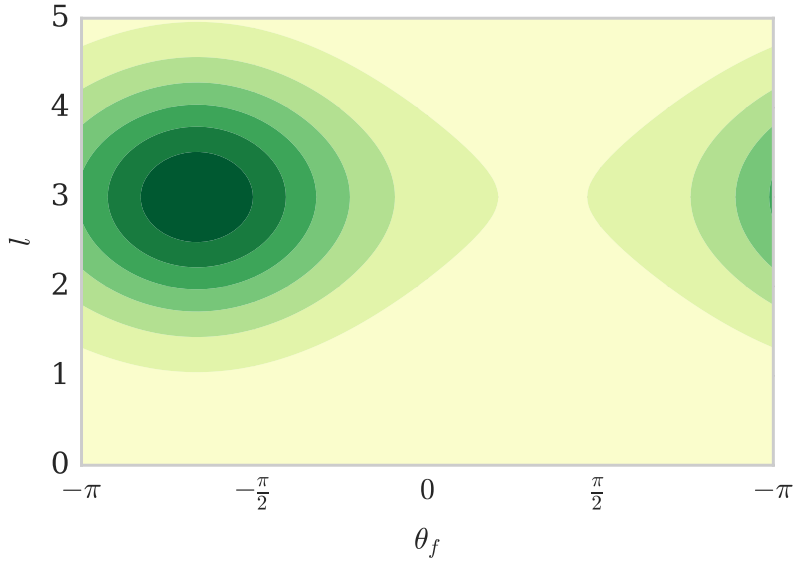

Figure 2.5: 2D length-angle probability distribution with $\theta_w = 2\pi/3, v_w = 1$

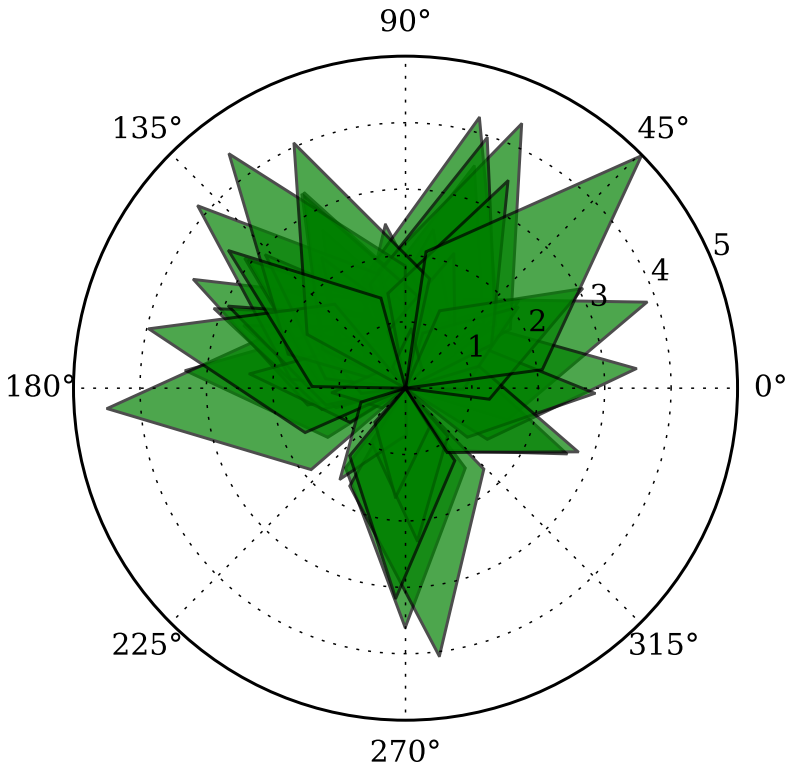

Figure 2.6: A sample of 50 kelp fronds with length and angle picked from the distribution above with $f_s = 0.5$ and $f_r = 2$.

CHAPTER III

LIGHT MODEL

Now that we have formulated the distribution of kelp throughout the medium, we introduce the radiative transfer equation, which is used to calculate the light field.

3.0.1 Optical Definitions

One of the most fundamental quantities in optics is radiant flux Φ, which is the has units of energy per time. The quantity of primary interest in modeling the light field is radiance L, which is defined as the radiant flux per steradian per projected surface area perpendicular to the direction of propagation of the beam. That is,

$$L = \frac{d^2\Phi}{dAd\omega} \tag{3.1}$$

We must now define a few inherent optical properties (IOPs) which depend only on the medium of propagation.

3.0.2 Characteristic Rays

Consider a fixed position $\vec{x}$ and direction $\vec{\omega}$ such that $\vec{\omega} \cdot \hat{z} \neq 0$.

Let $\vec{l}(\vec{x}, \vec{\omega}, s)$ denote the linear path containing $\vec{x}$ with initial z coordinate given by

$$z_0 = \begin{cases} 0, & \vec{\omega} \cdot \hat{z} < 0 \\ z_{\max}, & \vec{\omega} \cdot \hat{z} > 0 \end{cases} \tag{3.2}$$

Then,

$$\vec{l}(\vec{x}, \vec{\omega}, s) = \frac{1}{\tilde{s}}(s\vec{x} + (\tilde{s} - s)\vec{x_0}(\vec{x}, \vec{\omega})) \tag{3.3}$$

where

$$\vec{x_0}(\vec{x}, \vec{\omega}) = \vec{x} - \tilde{s}\vec{\omega} \tag{3.4}$$

is the origin of the ray, and

$$\tilde{s} = \frac{\vec{x} \cdot \hat{z} - z_0}{\vec{\omega} \cdot \hat{z}} \tag{3.5}$$

is the path length from $\vec{x_0}(\vec{x}, \vec{\omega})$ to $\vec{x}$.

3.0.3 Colloquial Description

Denote the radiance at $\vec{x}$ in the direction $\vec{\omega}$ by $L(\vec{x}, \vec{\omega})$. As light travels along $\vec{l}(\vec{x}, \vec{\omega}, s)$, interaction with the medium produces three phenomena of interest:

1. Radiance is decreased due to absorption.

2. Radiance is decreased due to scattering out of the path to other directions.

3. Radiance is increased due to scattering into the path from other directions.

3.0.4 IOPs

These phenomena are governed by three inherent optical properties (IOPs) of the medium. The absorption coefficient $a(\vec{x})$ (units m^{-1}) defines the proportional loss of radiance per unit length. The scattering coefficient b (units m^{-1}), defines the proportional loss of radiance per unit length, and is assumed to be constant over space.

The volume scattering function (VSF) $\beta(\Delta) : [-1, 1] \to \mathbb{R}^+$ (units sr^{-1}) defines the probability of light scattering at any given angle from its source. Formally, given two directions $\vec{\omega}$ and $\vec{\omega}'$, $\beta(\vec{\omega} \cdot \vec{\omega}')$ is the probability density of light scattering from $\vec{\omega}$ into $\vec{\omega}'$ (or vice-versa). Of course, since a single direction subtends no solid angle, the probability of scattering occuring exactly from $\vec{\omega}$ to $\vec{\omega}'$ is 0. Rather, we say that the probability of radiance being scattered from a direction ω into an element of solid angle Ω is $\int_\Omega \beta(\vec{\omega} \cdot \vec{\omega}')\, d\vec{\omega}'$.

The VSF is normalized such that

$$\int_{-1}^{1} \beta(\Delta)\, d\Delta = \frac{1}{2\pi}, \tag{3.6}$$

so that for any ω,

$$\int_{4\pi} \beta(\vec{\omega} \cdot \vec{\omega}')\, d\vec{\omega}' = 1. \tag{3.7}$$

i.e., the probability of light being scattered to some direction on the unit sphere is 1.

3.0.5 Equation of Transfer

Then, combining these phenomena, the Radiative Transfer equation along $\vec{l}(\vec{x},\vec{\omega})$ becomes

$$\frac{dL}{ds}(\vec{l}(\vec{x},\vec{\omega},s),\vec{\omega}) = -(a(\vec{x})+b)L(\vec{x},\vec{\omega}) + b\int_{4\pi}\beta(\vec{\omega}\cdot\vec{\omega}')L(\vec{x})\,d\omega', \tag{3.8}$$

where $\int_{4\pi}$ denotes integration over the unit sphere.

Now, we have

$$\begin{aligned}\frac{dL}{ds}(\vec{l}(\vec{x},\vec{\omega},s),\vec{\omega}) &= \frac{d\vec{l}}{ds}(\vec{x},\vec{\omega},s)\cdot\nabla L(\vec{x},\vec{\omega}',\vec{\omega}) \\ &= \vec{\omega}\cdot\nabla L(\vec{x},\vec{\omega})\end{aligned}$$

Then, the general form of the Radiative Transfer Equation is

$$\vec{\omega}\cdot\nabla L(\vec{x},\vec{\omega}) = -(a(\vec{x})+b)L(\vec{x},\vec{\omega}) + b\int_{4\pi}\beta(\vec{\omega}\cdot\vec{\omega}')L(\vec{x},\vec{\omega}')\,d\omega' \tag{3.9}$$

or, equivalently,

$$\vec{\omega}\cdot\nabla L(\vec{x},\vec{\omega}) + a(\vec{x})L(\vec{x},\vec{\omega}) = b\left(\int_{4\pi}\beta(\vec{\omega}\cdot\vec{\omega}')L(\vec{x},\vec{\omega}')\,d\omega' - L(\vec{x},\vec{\omega})\right) \tag{3.10}$$

3.0.6 Boundary Conditions

We use periodic boundary conditions in the x and y directions.

$$L\left((x_{\min},y,z),\vec{\omega}\right) = L\left((x_{\max},y,z),\vec{\omega}\right) \tag{3.11}$$

$$L\left((x,y_{\min},z),\vec{\omega}\right) = L\left((x,y_{\max},z),\vec{\omega}\right) \tag{3.12}$$

In the z direction, we specify a spatially uniform downwelling light just under the surface of the water by a function $f(\vec{\omega})$. Or if $z_{\min} > 0$, then the radiance at

$z = z_{\min}$ should be specified instead (as opposed to the radiance at the first grid cell center).

Further, we assume that no upwelling light enters the domain from the bottom.

$$L(\vec{x_s}, \vec{\omega}) = f(\omega) \text{ if } \vec{\omega} \cdot \hat{z} > 0 \tag{3.13}$$

$$L(\vec{x_b}, \vec{\omega}) = 0 \text{ if } \vec{\omega} \cdot \hat{z} < 0 \tag{3.14}$$

3.1 Irradiance

Once the radiance L is calculated everywhere, the irradiance is

$$I(\vec{x}) = \int_{4\pi} L(\vec{x}, \vec{\omega})\, d\omega. \tag{3.15}$$

Integrating $I(\vec{x})$, which has units $\mathrm{W/m^2}$, over the surface of a frond, produces the power (with units W) transmitted to the frond. This is discussed further in Section **??** This can be converted to moles of photons (also called einsteins) per second as

$$1\,\mathrm{W/m^2} = 4.2\,\mu\mathrm{mol\,photons/s}. \tag{3.16}$$

3.2 Asymptotics

In clear waters where absorption is more important than scattering, an asymptotic expansion can be used whereby the light field is generated through a sequence of discrete scattering events.

3.2.1 Substitute asymptotic series

Taking b to be small, we introduce the asymptotic series

$$L(\vec{x},\vec{\omega}) = L_0(\vec{x},\vec{\omega}) + bL_1(\vec{x},\vec{\omega}) + b^2L_2(\vec{x},\vec{\omega}) + \cdots . \tag{3.17}$$

Then, substituting the above into the RTE,

$$\begin{aligned}
&\vec{\omega}\cdot\nabla\left[L_0(\vec{x},\vec{\omega}) + bL_1(\vec{x},\vec{\omega}) + b^2L_2(\vec{x},\vec{\omega}) + \cdots\right] \\
&+ a(\vec{x})\left[L_0(\vec{x},\vec{\omega}) + bL_1(\vec{x},\vec{\omega}) + b^2L_2(\vec{x},\vec{\omega}) + \cdots\right] \\
&= b\Bigg(\int_{4\pi}\beta(|\vec{\omega}-\vec{\omega}'|)\left[L_0(\vec{x},\vec{\omega}') + bL_1(\vec{x},\vec{\omega}') + b^2L_2(\vec{x},\vec{\omega}') + \cdots\right]d\vec{\omega}' \\
&- \left[L_0(\vec{x},\vec{\omega}) + bL_1(\vec{x},\vec{\omega}) + b^2L_2(\vec{x},\vec{\omega}) + \cdots\right]\Bigg)
\end{aligned} \tag{3.18}$$

Then, grouping like powers of b, we have the decoupled set of equations

$$\vec{\omega}\cdot\nabla L_0(\vec{x},\vec{\omega}) + a(\vec{x})L_0(\vec{x}) = 0 \tag{3.19}$$

$$\vec{\omega}\cdot\nabla L_1(\vec{x},\vec{\omega}) + a(\vec{x})L_1(\vec{x}) = \int_{4\pi}\beta(|\vec{\omega}-\vec{\omega}'|)L_0(\vec{x},\vec{\omega}')\,d\vec{\omega}' - L_0(\vec{x},\vec{\omega}) \tag{3.20}$$

$$\vec{\omega}\cdot\nabla L_2(\vec{x},\vec{\omega}) + a(\vec{x})L_2(\vec{x}) = \int_{4\pi}\beta(|\vec{\omega}-\vec{\omega}'|)L_1(\vec{x},\vec{\omega}')\,d\vec{\omega}' - L_1(\vec{x},\vec{\omega}) \tag{3.21}$$

$$\vdots$$

For boundary conditions, let x_s be a point on the surface of the domain. Then,

$$L_0(\vec{x_s},\vec{\omega}) + bL_1(\vec{x_s},\vec{\omega}) + b^2L_2(\vec{x_s},\vec{\omega}) + \cdots = \begin{cases} f(\omega), & \hat{z}\cdot\omega > 0 \\ 0, & \text{otherwise,} \end{cases} \tag{3.22}$$

which becomes

$$L_0(\vec{x},\vec{\omega}) = \begin{cases} f(\omega), & \hat{z}\cdot\omega > 0, \\ 0, & \text{otherwise}, \end{cases} \tag{3.23}$$

$$L_1(\vec{x},\vec{\omega}) = 0 \tag{3.24}$$

$$L_2(\vec{x},\vec{\omega}) = 0. \tag{3.25}$$

$$\vdots$$

3.2.2 Rewrite as ODE along ray path

For all $\vec{x},\vec{\omega}$, let

$$\tilde{a}(s) = a(\vec{l}(\vec{x},\vec{\omega}),s), \tag{3.26}$$

$$\frac{du_0}{ds}(s) + \tilde{a}(s)u_0(s) = 0, u_0(0) = f(\vec{\omega}) \tag{3.27}$$

Then,

$$u_0(s) = f(\omega)\exp\left(-\int_0^s \tilde{a}(s)\,ds\right), \tag{3.28}$$

$$L_0(\vec{l}(\vec{x},\vec{\omega},s),\vec{\omega}) = u_0(s) \tag{3.29}$$

$$g_n(s) = \int_{4\pi} \beta(|\vec{\omega}-\vec{\omega}'|)L_{n-1}(\vec{l}(\vec{x},\vec{\omega'},s),\vec{\omega}')\,d\vec{\omega}' - L_{n-1}(\vec{l}(\vec{x},\vec{\omega},s),\vec{\omega}) \tag{3.30}$$

$$\frac{du_n}{ds}(s) + \tilde{a}(s)u_n(s) = g_n(s), u_n(0) = 0 \tag{3.31}$$

Then,

$$u_n(s) = \int_0^s g_n(s') \exp\left(- \int_{s''}^{s'} \tilde{a}(s'')\, ds'' \right) ds' \tag{3.32}$$

$$L_n(\vec{l}(\vec{x}, \vec{\omega}, s), \vec{\omega}) = u_n(s) \tag{3.33}$$

CHAPTER IV

PARAMETER VALUES

I'll describe what one would do in order to determine "frond bending coefficients", as well as optical properties of water and kelp, citing literature and reporting values obtained by others.

4.1 Parameters from Literature

* More to come

4.2 Optical Properties

4.2.1 Absorption Coefficients

4.2.2 Scattering Coefficients

4.2.3 Volume Scattering Function

4.3 Frond Distribution Parameters

4.3.1 Rotation

4.3.2 Lift

Parameter Name	Symbol	Value(s)	Citation	Notes
Kelp Absorptance	A_k	0.8	[4]	Actually for *Macrocystis Pyrifera*
Water absorption coefficient	a_w	?	?	?
Scattering coefficient	b	0.366	[11]	Table 2, $b_{\lambda 0}$, mean
VSF	β	tabulated	[10, 11],	Currently using Petzold
Frond thickness	t	0.4 mm	Ole Jacob	Carina? ***
Water absorption coefficient	a_w	0.03 1 1/m	[6]	Fig. 6, dense cluster. Samnanger Fjord, Western Norway.
Water scattering coefficient	a_w	0.5 1 1/m	[6]	Fig. 7, dense cluster. Samnanger Fjord, Western Norway.
Surface solar irradiance	I_0	50 W m^{-2}	[2]	Irradiance for maximal photosynthesis, converted from photons

Site	$a(\mathbf{m^{-1}})$	$b(\mathbf{m^{-1}})$	$c(\mathbf{m^{-1}})$	a/c	b/c
AUTEC 7	0.082	0.117	0.199	0.412	0.588
AUTEC 8	0.114	0.037	0.151	0.753	0.247
AUTEC 9	0.122	0.043	0.165	0.742	0.258
HAOCE 5	0.195	0.275	0.47	0.415	0.585
HAOCE 11	0.179	0.219	0.398	0.449	0.551
NUC 2200	0.337	1.583	1.92	0.176	0.824
NUC 2040	0.366	1.824	2.19	0.167	0.833
NUC 2240	0.125	1.205	1.33	0.094	0.906
Filtered Fresh	0.093	0.009	0.102	0.907	0.093
Filtered Fresh + Scat.	0.138	0.547	0.685	0.202	0.798
Fresh + Scat. + Abs.	0.764	0.576	1.34	0.57	0.43
As Delivered	0.196	1.284	1.48	0.133	0.867
Filtered 40 min	0.188	0.407	0.595	0.315	0.685
Filtered 1hr 40 min	0.093	0.081	0.174	0.537	0.463
Filtered 18hr	0.085	0.008	0.093	0.909	0.091

Table 4.2: Petzold IOP summary

CHAPTER V

MODEL ANALYSIS

5.1 Grid Study

Run many grid sizes with GMRES, using asymptotic solution as initial guess. Compare CPU times and accuracy, assuming largest grid is "true" solution. Determine necessary grid size to achieve reasonable accuracy.

5.2 Asymptotics vs. Finite Difference

Compare asymptotic solutions to GMRES with reasonable grid size as determined above. Compare CPU time and accuracy. Determine ideal number of scatters to include (number of terms in asymptotic series). Repeat for a few values of scattering coefficient.

5.3 Sensitivity analysis

Vary parameters and measure average differences in radiance for full grid, as well as average irradance over depth.

- absorption coefficient
- scattering coefficient

- VSF

- frond bending coefficient

5.4 Lifecycle Simulation

Run Ole Jacob's model with my new light model, compare:

- irrad over time for several depths

- computation time

- harvestable biomass

CHAPTER VI

CONCLUSION

We present a probabilistic model for the spatial distribution of kelp, and develop a first-principles model for the light field, considering absorption and scattering due to the water and kelp. A full finite difference solution is presented, and an asymptotic approximation based on discrete scattering events is subsequently developed.

Future work:

- Frond bending
- Horizontal kelp ropes (long lines)
- etc.

BIBLIOGRAPHY

[1] N. Anderson. A mathematical model for the growth of giant kelp. *Simulation*, 22(4):97–105, 1974.

[2] O. J. Broch and D. Slagstad. Modelling seasonal growth and composition of the kelp Saccharina latissima. *Journal of Applied Phycology*, 24(4):759–776, Aug. 2012.

[3] M. A. Burgman and V. A. Gerard. A stage-structured, stochastic population model for the giant kelpMacrocystis pyrifera. *Marine Biology*, 105(1):15–23, 1990.

[4] M. F. Colombo-Pallotta, E. Garca-Mendoza, and L. B. Ladah. Photosynthetic Performance, Light Absorption, and Pigment Composition of Macrocystis Pyrifera (laminariales, Phaeophyceae) Blades from Different Depths1. *Journal of Phycology*, 42(6):1225–1234, Dec. 2006.

[5] P. Duarte and J. G. Ferreira. A model for the simulation of macroalgal population dynamics and productivity. *Ecological modelling*, 98(2-3):199–214, 1997.

[6] B. Hamre, . Frette, S. R. Erga, J. J. Stamnes, and K. Stamnes. Parameterization and analysis of the optical absorption and scattering coefficients in a western

Norwegian fjord: a case II water study. *Applied Optics*, 42(6):883, Feb. 2003.

[7] G. A. Jackson. Modelling the growth and harvest yield of the giant kelp Macrocystis pyrifera. *Marine Biology*, 95(4):611–624, 1987.

[8] C. Mobley. Radiative Transfer in the Ocean. In *Encyclopedia of Ocean Sciences*, pages 2321–2330. Elsevier, 2001.

[9] M. Nyman, M. Brown, M. Neushul, and J. A. Keogh. *Macrocystis pyrifera in New Zealand: testing two mathematical models for whole plant growth*, volume 2. Sept. 1990.

[10] T. J. Petzold. Volume Scattering Function for Selected Ocean Waters. Technical report, DTIC Document, 1972.

[11] A. Sokolov, M. Chami, E. Dmitriev, and G. Khomenko. Parameterization of volume scattering function of coastal waters based on the statistical approach. *Optics express*, 18(5):4615–4636, 2010.

[12] P. Wassmann, D. Slagstad, C. W. Riser, and M. Reigstad. Modelling the ecosystem dynamics of the Barents Sea including the marginal ice zone. *Journal of Marine Systems*, 59(1-2):1–24, Jan. 2006.

[13] A. Yoshimori, T. Kono, and H. Iizumi. Mathematical models of population dynamics of the kelp Laminaria religiosa, with emphasis on temperature dependence. *Fisheries Oceanography*, 7(2):136146, 1998.